Self-Consistent Tensor Product Variational Approximation for 3D Classical Models

T. Nishino [a] K. Okunishi [b] Y. Hieida [c,d] N. Maeshima [d]
Y. Akutsu [d]

[a] *Department of Physics, Faculty of Science, Kobe University, 657-8501, Japan*

[b] *Department of Applied Physics, Graduate school of Engineering, Osaka University, Suita 575-0871, Japan*

[c] *Computer Center, Gakushuin University, Toshima-ku, Tokyo 171-8588, Japan*

[d] *Department of Physics, Graduate School of Science, Osaka University, Toyonaka 560-0043, Japan*

Abstract

We propose a numerical variational method for three-dimensional (3D) classical lattice models. We construct the variational state as a product of local tensors, and improve it by use of the corner transfer matrix renormalization group (CTMRG), which is a variant of the density matrix renormalization group (DMRG) applied to 2D classical systems. Numerical efficiency of this approximation is investigated through trial applications to the 3D Ising model and the 3D 3-state Potts model.

Key words: DMRG; CTMRG; Variational Formulation

1 Introduction

The density matrix renormalization group (DMRG) [1,2] has been widely applied to one-dimensional (1D) quantum systems and two-dimensional (2D) classical systems [3,4]. A frontier in DMRG is to extend its numerical algorithm to higher dimensional systems, chiefly for 2D quantum and 3D classical systems. As far as the finite system algorithm is concerned, decomposition of higher-dimensional clusters to 1D chains proposed by Liang and Pang works efficiently [5]. On the other hand, we have not obtained any satisfactory answer to extend DMRG toward infinite-size systems in higher dimension. Nishino and Okunishi proposed a way of extending DMRG to 3D classical systems, which they call 'the corner tensor renormalization group (CTTRG)' [6], as a 3D generalization of both the transfer matrix DMRG [3,7] and the corner transfer

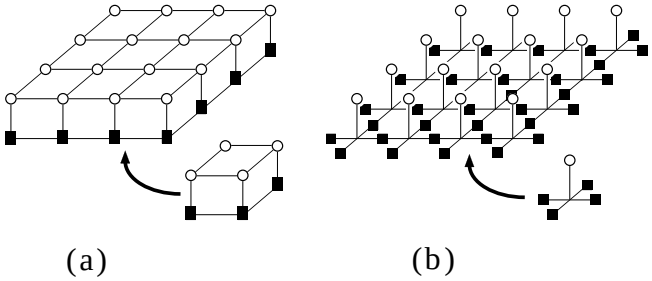

Fig. 1. Two representative constructions of the tensor product variational state: (a) the IRF type and (b) the vertex type. The white circles denote spin (or field) variables, and the black squares denote auxiliary variables. We consider the simplest example of the (a)-type product state in this paper.

matrix renormalization group (CTMRG) [8,9] for 2D classical systems. Two major problems are found in CTTRG when it is applied to the 3D Ising model. One is that the calculated transition temperature $T_{\rm c}$ is much higher than one of the most reliable $T_{\rm c}$ obtained with the Monte Carlo (MC) simulations [10,11]. The other problem is the very slow decay of the the density-matrix eigenvalues [12], that spoils the numerical efficiency of the block-spin transformation.

Another way of generalizing DMRG to higher dimensions is to investigate the variational structure of DMRG, where the variational state for the transfer matrix or the Hamiltonian is written in a product of orthogonal matrices [13]. Two types of 2D tensor product states have been considered as higher-dimensional extensions of this matrix product state. One is 'the interaction round a face (IRF)' type product states shown in figure (1(a)) [14], and the other is the vertex type one in figure (1(b)) [15,16]. For a 2D tensor product state V, the variational energy and the variational partition function, respectively, is written as

$$\lambda = \frac{\langle V|\, H\, |V\rangle}{\langle V|V\rangle} \quad \text{and} \quad \frac{\langle V|\, T\, |V\rangle}{\langle V|V\rangle}\,, \tag{1}$$

where H and T denotes a Hamiltonian for a 2D quantum system and a transfer matrix for a 3D classical system. Let us call such a variational estimation as 'the tensor product variational approximation (TPVA)' in the following. Calculation of λ have been performed by MC simulation [15], product wave function renormalization group (PWFRG) [16] or CTMRG [18]. A key point in TPVA is to find a good variational state V. So far, they assumed a specific form of V, which contains several variational parameters, and tried to find out the best V by way of the parameter sweep. For example, Okunishi and Nishino [18] investigated TPVA for the 3D Ising model, assuming V in the form of the Kramers-Wannier (KW) approximation [17]. Their variational state contains two adjustable parameters, and the best V is obtained through a two-parameter sweep. Such an intuitive construction of V is, however, not always

applicable; for example, we don't know how to extend the KW approximation for the 3D Potts models [19]. How can we obtain the best V automatically for higher-dimensional systems? We find an answer for 3D classical systems.

In this paper we propose a self-consistent improvement for the tensor product state V by way of CTMRG. We choose the 3D Ising model as an example of the 3D classical systems, and formulate our self-consistent method in terms of the Ising model. In the next section, we introduce the simplest 2D tensor product state, and give the formal expression of the variational partition function λ in eq.(1). We then obtain the self-consistent equation for V in §3, considering the variation $\delta\lambda/\delta V$. In §4 we propose a numerical algorithm to solve the self-consistent equation. In §5 we check the numerical efficiency and stability of this algorithm when it is applied to the 3D Ising model and the 3-state ($q = 3$) 3D Potts model. Conclusions are summarized in §6.

2 Tensor Product Variational State

We briefly review the variational formulation of TPVA that was used for the KW approximation of the 3D Ising model [18]. Let us consider the 3D Ising model on the simple cubic lattice of the size $2N \times 2N \times \infty$ to X, Y and Z directions, respectively, where open (or fixed) boundary conditions are assumed for both X and Y directions. We are interested in the bulk property of this model, and therefore suppose that the system size $2N$ is sufficiently large. Suppose that the neighboring Ising spins σ and σ' have ferromagnetic interaction $-J\sigma\sigma'$. The transfer matrix T from a $2N \times 2N$ spin layer

$$[\sigma] \equiv \begin{bmatrix} \sigma_{1\,1} & \cdots & \sigma_{1\,N} & \cdots & \sigma_{1\,2N} \\ \vdots & \ddots & \vdots & \ddots & \vdots \\ \sigma_{N\,1} & \cdots & \sigma_{N\,N} & \cdots & \sigma_{N\,2N} \\ \vdots & \ddots & \vdots & \ddots & \vdots \\ \sigma_{2N\,1} & \cdots & \sigma_{2N\,N} & \cdots & \sigma_{2N\,2N} \end{bmatrix} \tag{2}$$

to the next layer $[\bar{\sigma}]$ is then expressed as a product of local factors

$$T[\bar{\sigma}|\sigma] = \prod_{i=1}^{2N-1} \prod_{j=1}^{2N-1} X_{ij} \equiv \prod_{ij} X_{ij}\,, \tag{3}$$

where X_{ij} represents the Boltzmann factor for a local cube

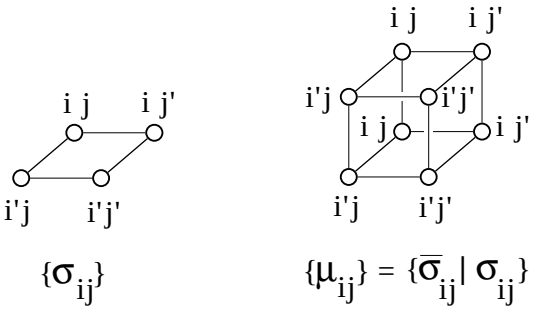

Fig. 2. Positions of the spin variables. The plaquett spin $\{\sigma_{ij}\}$ in eq.(6) consists of 4 neighboring spins, where $i' = i + 1$ and $j' = j + 1$, and the cube spin $\{\mu_{ij}\}$ in eq.(15) consists of a stack of two plaquett spins $\{\bar{\sigma}_{ij}\}$ and $\{\sigma_{ij}\}$.

$$X_{ij} = \exp\Big\{\frac{K}{4}\big(\bar{\sigma}_{i'j}\bar{\sigma}_{ij}+\bar{\sigma}_{ij'}\bar{\sigma}_{ij}+\bar{\sigma}_{i'j'}\bar{\sigma}_{i'j}+\bar{\sigma}_{i'j'}\bar{\sigma}_{ij'} \tag{4}$$
$$+\bar{\sigma}_{ij}\sigma_{ij}+\bar{\sigma}_{i'j}\sigma_{i'j}+\bar{\sigma}_{ij'}\sigma_{ij'}+\bar{\sigma}_{i'j'}\sigma_{i'j'}$$
$$+\sigma_{i'j}\sigma_{ij}+\sigma_{ij'}\sigma_{ij}+\sigma_{i'j'}\sigma_{i'j}+\sigma_{i'j'}\sigma_{ij'}\big)\Big\}$$

parameterized by $K = J/k_{\rm B}T$. We have used the notation $i' = i + 1$ and $j' = j + 1$. (See figure (2).) We define $T[\bar{\sigma}|\sigma]$ so that it is symmetric, because the symmetry simplifies the following formulation.

The variational state in TPVA is a uniform product of local tensors. In this paper, we focus on the simplest construction of the tensor product state

$$V[\sigma] = \prod_{ij} W_{ij} = \prod_{ij} W \begin{pmatrix} \sigma_{ij} & \sigma_{ij'} \\ \sigma_{i'j} & \sigma_{i'j'} \end{pmatrix}, \tag{5}$$

where the local tensor W_{ij} does not contains auxiliary variables, which are shown by black squares in figure (1(a)) [16,14]; to include the auxiliary variables is straightforward, but makes the following equations rather lengthy. The tensor product state $V[\sigma]$ is uniform in the sense that W_{ij} is position independent. The local tensor W_{ij} has 16 parameters, but not all of them are physically independent [20]. For the book keeping, let us use the notation

$$\{\sigma_{ij}\} \equiv \begin{pmatrix} \sigma_{ij} & \sigma_{ij'} \\ \sigma_{i'j} & \sigma_{i'j'} \end{pmatrix} \tag{6}$$

for the plaquett spin, and write the local tensor W_{ij} simply as $W\{\sigma_{ij}\}$. In the same manner, let us write X_{ij} as $X\{\bar{\sigma}_{ij}|\,\sigma_{ij}\}$. (See figure (2).)

Using $T[\bar{\sigma}|\sigma]$ and $V[\sigma]$ thus defined, the variational partition function per layer is expressed as

$$\lambda = \frac{\sum_{[\bar{\sigma}][\sigma]} V[\bar{\sigma}]\, T[\bar{\sigma}|\sigma]\, V[\sigma]}{\sum_{[\sigma]} (V[\sigma])^2} = \frac{\sum_{[\bar{\sigma}][\sigma]} \prod_{ij} W\{\bar{\sigma}_{i\,j}\}\, X\{\bar{\sigma}_{ij}|\, \sigma_{ij}\}\, W\{\sigma_{i\,j}\}}{\sum_{[\sigma]} \prod_{ij} \Big(W\{\sigma_{i\,j}\}\Big)^2}$$
$$= \frac{\sum_{[\bar{\sigma}][\sigma]} \prod_{ij} G^1\{\bar{\sigma}_{ij}|\, \sigma_{ij}\}}{\sum_{[\sigma]} \prod_{ij} G^0\{\sigma_{ij}\}} \equiv \frac{Z^1}{Z^0}\,, \tag{7}$$

where we have defined G^0 and G^1 as

$$G^0\{\sigma_{ij}\} = \Big(W\{\sigma_{i\,j}\}\Big)^2\,,$$
$$G^1\{\bar{\sigma}_{ij}|\, \sigma_{ij}\} = W\{\bar{\sigma}_{i\,j}\}\, X\{\bar{\sigma}_{ij}|\, \sigma_{ij}\}\, W\{\sigma_{i\,j}\}\,. \tag{8}$$

It should be noted that Z^0 is a partition function of an IRF model [20] on $2N \times 2N$ square, and Z^1 is that of a 2-layer lattice model of the same size.

3 Self-Consistent Relation for the variational state

Now we explain the self-consistent equation for the variational state $V[\sigma]$, the equation which is satisfied when λ in eq.(7) is maximized. Let us consider the variation of λ with respect to the variations of local tensors

$$\frac{\delta\,\lambda}{\delta\, V} \equiv \sum_{ij} \frac{\delta\,\lambda}{\delta\, W_{ij}} \tag{9}$$

under the condition that the system size $2N$ is sufficiently large and the boundary effect is negligible. Then most of the terms in the r.h.s. are almost the same, and it is sufficient to consider the variation of λ with respect to the local change $W_{NN} \to W_{NN} + \delta\, W_{NN}$ at the center of the system, where W_{NN} represents the local tensor at the center. (See eqs.(2) and (5).)

The variation $\delta\,\lambda/\delta\, W_{NN}$ can be explicitly written down by use of two matrices. One is the diagonal matrix

$$A\{\sigma_{NN}\} = \sum_{[\sigma]'} \prod_{(ij)\neq(NN)} G^0\{\sigma_{ij}\}\,, \tag{10}$$

where $\sum_{[\sigma]'}$ denotes spin configuration sum for all the spins in the layer $[\sigma]$ except for the spin plaquett $\{\sigma_{NN}\}$ at the center; we interpret $A\{\sigma_{NN}\}$ as a 16-dimensional matrix $M\{\bar{\sigma}_{NN}|\sigma_{NN}\}$ where $M\{\sigma_{NN}|\sigma_{NN}\} = A\{\sigma_{NN}\}$ and is zero when $\{\bar{\sigma}_{NN}\} \neq \{\sigma_{NN}\}$. From the definition, Z^0 in eq.(7) is equal to $\sum_{\{\sigma_{NN}\}} G^0\{\sigma_{NN}\}A\{\sigma_{NN}\}$. The other matrix is

$$B\{\bar{\sigma}_{NN}|\sigma_{NN}\} = X\{\bar{\sigma}_{NN}|\sigma_{NN}\} \sum_{[\bar{\sigma}]'[\sigma]'} \prod_{(ij)\neq(NN)} G^1\{\bar{\sigma}_{ij}|\,\sigma_{ij}\}\,, \tag{11}$$

which is related to Z^1 as $Z^1 = \sum_{\{\bar{\sigma}_{NN}\}\{\sigma_{NN}\}} W\,\{\bar{\sigma}_{NN}\}B\{\bar{\sigma}_{NN}|\sigma_{NN}\}W\{\sigma_{NN}\}$. By use of $A\{\sigma_{NN}\}$ and $B\{\bar{\sigma}_{NN}|\sigma_{NN}\}$ thus created, we can write down λ as

$$\lambda = \frac{Z^1}{Z^0} = \frac{\sum_{\{\bar{\sigma}\}\{\sigma\}} W\{\bar{\sigma}\}\,B\{\bar{\sigma}|\sigma\}\,W\{\sigma\}}{\sum_{\{\sigma\}} W\{\sigma\}\,A\{\sigma\}\,W\{\sigma\}}\,, \tag{12}$$

where we have dropped the subscripts from $\{\sigma_{NN}\}$ and $\{\bar{\sigma}_{NN}\}$ for book keeping. The condition $\delta\,\lambda/\delta\,W\{\sigma_{NN}\} = 0$ draws the eigenvalue problem

$$\sum_{\{\sigma\}} \frac{1}{A\{\bar{\sigma}\}}\,B\{\bar{\sigma}|\sigma\}\,W\{\sigma\} = \lambda\,W\{\bar{\sigma}\} \tag{13}$$

between the matrix $A^{-1}B$ and W; here we regard $W\{\sigma\}$ as a 16-dimensional vector. This is the self-consistent equation that an optimized tensor product state $V[\sigma]$ should satisfy.

4 Numerical Algorithm of the Self-Consistent TPVA

To use the self-consistent relation eq.(13), we have to obtain $A\{\sigma\}$ and $B\{\bar{\sigma}|\sigma\}$ for very large N. Though it is impossible to obtain $A\{\sigma\}$ and $B\{\bar{\sigma}|\sigma\}$ exactly, the CTMRG [8,9] enables us to numerically obtain them very accurately. Let us introduce a new notation

$$\mu_{ij} \equiv \left(\bar{\sigma}_{ij}, \sigma_{ij}\right)\,, \tag{14}$$

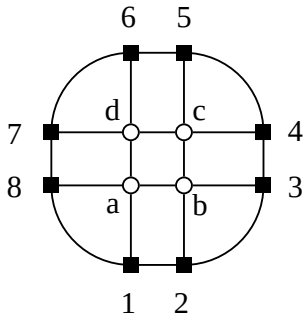

Fig. 3. Positions of the spin variables in eqs.(16). The four white circles denote the plaquett spin $\{\sigma\}$ or $\{\mu\}$ at the center, and the black squares denote the block-spin variables used in CTMRG.

which groups a pair of adjacent spins $\bar{\sigma}_{ij}$ and σ_{ij}. Using μ_{ij}, we can rewrite the stack of two plaquett spins $\{\bar{\sigma}_{ij}|\sigma_{ij}\}$ as

$$\{\mu_{i\,j}\} = \begin{pmatrix} \mu_{i\,j} & \mu_{i\,j'} \\ \mu_{i'j} & \mu_{i'j'} \end{pmatrix}, \tag{15}$$

$X\{\bar{\sigma}_{ij}|\,\sigma_{ij}\}$ as $X\{\mu_{ij}\}$, and $G^1\{\bar{\sigma}_{ij}|\,\sigma_{ij}\}$ as $G^1\{\mu_{ij}\}$. (See figure (2)) We drop the subscripts from $\{\mu_{i\,j}\}$ to write it as $\{\mu\}$ when its position is apparent.

The matrices $A\{\sigma\}$ and $B\{\mu\} = B\{\bar{\sigma}|\sigma\}$ can be expressed as a combination of the corner transfer matrices (CTMs) and the half-row transfer matrices (HRTMs), that appears when we apply CTMRG to both the denominator and the numerator of eq.(7) to obtain Z^0 and Z^1 [18]. Let us write the CTM used for the calculation of Z^0 and Z^1, respectively, as $C^0(\xi\sigma\xi')$ and $C^1(\zeta\mu\zeta')$, where ξ, ξ', ζ, and ζ' are m-state block spin variables. Also let us write HRTM as $P^0(\xi\sigma\sigma'\xi')$ and $P^1(\zeta\mu\mu'\zeta')$ in the same manner. Note that $C^0(\xi\sigma\xi')$ and $P^0(\xi\sigma\sigma'\xi')$ are created from $G^0\{\sigma\}$, and $C^1(\zeta\mu\zeta')$ and $P^1(\zeta\mu\mu'\zeta')$ are from $G^1\{\mu\}$. Combining these CTMs and HRTMs, $A\{\sigma\}$ and $B\{\mu\}$ are constructed as

$$\begin{aligned} A\{\sigma\} = \sum_{\xi_1\cdots\xi_8} & P^0(\xi_1\sigma_a\sigma_b\xi_2)\,C^0(\xi_2\sigma_b\xi_3)\,P^0(\xi_3\sigma_b\sigma_c\xi_4)\,C^0(\xi_4\sigma_c\xi_5) \\ & P^0(\xi_5\sigma_c\sigma_d\xi_6)\,C^0(\xi_6\sigma_d\xi_7)\,P^0(\xi_7\sigma_d\sigma_a\xi_8)\,C^0(\xi_8\sigma_a\xi_1)\,, \\ B\{\mu\} = X\{\mu\}\sum_{\zeta_1\cdots\zeta_8} & P^1(\zeta_1\mu_a\mu_b\zeta_2)\,C^1(\zeta_2\mu_b\zeta_3)\,P^1(\zeta_3\mu_b\mu_c\zeta_4)\,C^1(\zeta_4\mu_c\zeta_5) \\ & P^1(\zeta_5\mu_c\mu_d\zeta_6)\,C^1(\zeta_6\mu_d\zeta_7)\,P^1(\zeta_7\mu_d\mu_a\zeta_8)\,C^1(\zeta_8\mu_a\zeta_1) \end{aligned} \tag{16}$$

where the positions of the spin variables are shown in figure (3). In principle, we can use $A\{\sigma\}$ and $B\{\mu\}$ thus constructed to solve the self-consistent eq.(13).

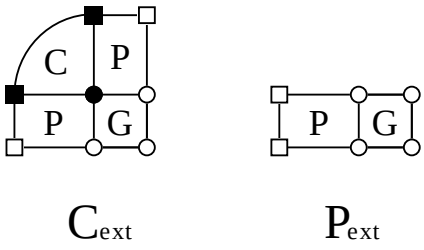

Fig. 4. Extension of CTM and HRTM [8,9]. The local factor G is created from the improved local tensor in eq.(18).

To make the self-consistent improvement for $W\{\sigma\}$ more efficiently, we employ a numerical algorithm that simultaneously performs the extension of the system size in CTMRG and the self-consistent improvement by eq.(13). The numerical procedures are as follows:

(a) Create $G^0\{\sigma\}$ and $G^1\{\mu\}$ from $X\{\mu\}$ defined in eq.(5) and the initial $W\{\sigma\}$:

$$\begin{aligned} G^0\{\sigma\} &= \left(W\{\sigma\}\right)^2 , \\ G^1\{\mu\} \equiv G^1\{\bar{\sigma}|\sigma\} &= W\{\bar{\sigma}\}\, X\{\bar{\sigma}|\ \sigma\}\, W\{\sigma\} . \end{aligned} \tag{17}$$

The choice of the initial $W\{\sigma\}$ is not so relevant, since it is improved afterward.

(b) Create the initial $C^0(\xi\sigma\xi')$ and the initial $P^0(\xi\sigma\sigma'\xi')$ from $G^0\{\sigma\}$, following the standard initialization procedure in CTMRG [8,9]. Also create $C^1(\zeta\mu\zeta')$ and $P^1(\zeta\mu\mu'\zeta')$ from $G^1\{\mu\}$ in the same way.

(c) Obtain the matrices $A\{\sigma\}$ and $B\{\mu\} = B\{\bar{\sigma}|\sigma\}$ using eqs.(16).

(d) Improve $W\{\sigma\}$ by multiplying $A^{-1}B$

$$\alpha W_{\rm new}\{\bar{\sigma}\} = \sum_{\{\sigma\}} \frac{1}{A\{\bar{\sigma}\}}\, B\{\bar{\sigma}|\sigma\}\, W_{\rm old}\{\sigma\} , \tag{18}$$

where α is an arbitrary constant which determines the normalization of $W_{\rm new}\{\bar{\sigma}\}$. We choose the normalization

$$\sum_{\{\sigma\}} \left(W_{\rm new}\{\sigma\}\right)^2 = 1 . \tag{19}$$

Note that when $W\{\sigma\}$ is optimized and $W\{\sigma\}_{\rm new} = W\{\sigma\}_{\rm old}$ is satisfied, α is equal to λ in eq.(7) under the normalization eq.(19).

(e) Recreate $G^0\{\sigma\}$ and $G^1\{\mu\}$ by substituting $W_{\rm new}\{\sigma\}$ into eqs.(17).

(f) Extend P^0 and P^1 to obtain $P^0_{\rm ext}$ and $P^1_{\rm ext}$, respectively, by joining the recreated G^0 and G^1 as shown in figure (4); the numerical details are shown in ref. [8,9]. Also extend C^0 and C^1 to obtain $C^0_{\rm ext}$ and $C^1_{\rm ext}$.

(g) Create density matrices from the extended CTMs, and diagonalizing them to obtain the RG transformations $\xi_{\rm old}\sigma \to \xi_{\rm new}$ and $\zeta_{\rm old}\mu \to \zeta_{\rm new}$, where ξ and ζ are m-state block spins. Then apply the RG transformations to $P^0_{\rm ext}$, $P^1_{\rm ext}$ $C^0_{\rm ext}$ and $C^1_{\rm ext}$.

(h) Goto (c), and repeat (c)-(g) to improve $W\{\sigma\}$ iteratively, and stop when $W\{\sigma\}$ reaches its fixed point.

To summarize, we put three additional steps (a), (c) and (d) to the standard CTMRG algorithm.

5 Numerical Results

Let us check the numerical efficiency and stability of the self-consistent TPVA through trial applications to the 3D Ising model and the ferromagnetic $q = 3$ Potts model. Figure (5) shows the spontaneous magnetization $\langle\sigma\rangle$ at the center of the $2N \times 2N \times \infty$ system, where the curve, cross marks, and triangles, respectively, represent the result of the MC simulation by Tarpov and Blöte [10], the KW approximation [18], and the self-consistent TPVA. We calculate $\langle\sigma\rangle$ after repeating the iteration (c)-(g) in the last section for $N = 10000$ times at most, keeping $m = 10$ to $m = 20$ states for the block spin variables; the convergence with respect to m is very fast, where we obtain almost the same $\langle\sigma\rangle$ for the cases $m = 10$ and 20. The self-consistent improvement by eq.(18) is monotonous in the whole parameter range, and no oscillatory instability is observed. The calculated magnetization behaves approximately as $6.372\sqrt{K - 0.2188}$ around the calculated transition point $K_{\rm c}^{\rm TPVA} = 0.2188$, and the observed phase transition is mean-field like. The transition point $K_{\rm c}^{\rm TPVA} = 0.2188$ is about 1.3% smaller than the MC result $K_{\rm c}^{\rm MC} = 0.2216544$. The transition point obtained with the KW approximation $K_{\rm c}^{\rm KW}$ is 0.2184, [18] and thus $K_{\rm c}^{\rm TPVA}$ is slightly larger than $K_{\rm c}^{\rm KW}$; in summary, $K_{\rm c}^{\rm KW} = 0.2184 < K_{\rm c}^{\rm TPVA} = 0.2188 < K_{\rm c}^{\rm MC} = 0.2216544$.

It turns out that the spontaneous magnetization calculated with the KW approximation is quite close to that calculated with the self-consistent TPVA. This suggests that the best variational state obtained with the KW approximation is quite close to that obtained with the self-consistent TPVA. We have actually confirmed that the local tensor in the KW approximation is very close to the $W\{\sigma\}$ in the self-consistent TPVA in the whole parameter region. Note that the computational time required for the KW approximation is several times larger than the self-consistent TPVA, because the former finds the partition function extremum via 2-parameter sweep.

Figure (6) shows the energy per bond $E = \langle -\delta(\sigma, \sigma')\rangle$ of the ferromagnetic 3D $q = 3$ Potts model, which is calculated by TPVA keeping m up to 15. The self-consistent improvement by eq.(18) is again monotonous, and $N = 1000$ is sufficient to get the converged data; we need smaller N for the Potts model than Ising model, because the phase transition of the Potts model is first order. The calculated energy per bond jumps from $E^+ = -0.5173$ to $E^- = -0.5933$

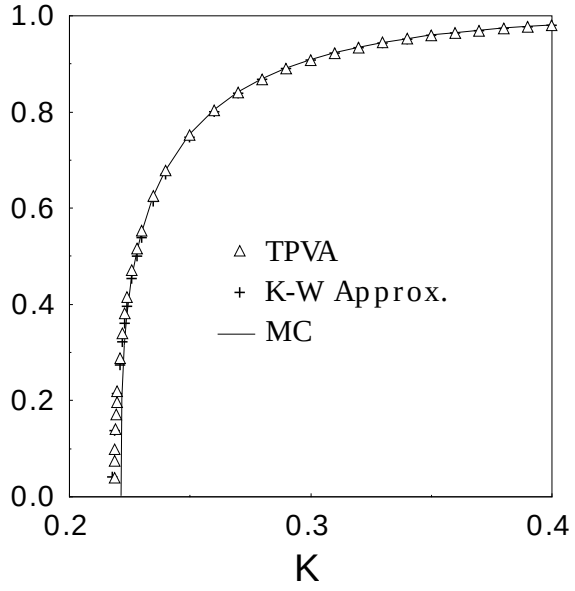

Fig. 5. Calculated spontaneous magnetization of the 3D Ising model.

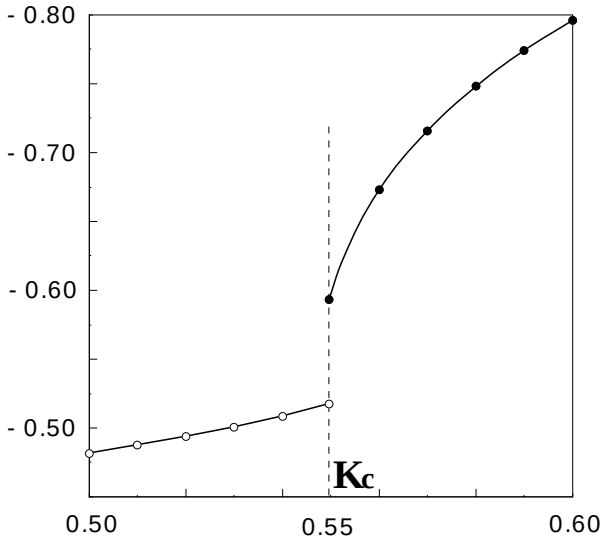

Fig. 6. Energy per bond $\langle -\delta(\sigma, \sigma') \rangle$ of the ferromagnetic 3D $q = 3$ Potts Model.

at the calculated transition point $K_{\rm c} = 0.54956$, where the calculated free energy of the disordered phase coincides with that of the ordered phase. The calculated transition point is about 0.18% smaller than one of the most reliable MC result $K_{\rm c}^{\rm MC} = 0.550565 \pm 0.000010$ [21]. The latent heat $l = 3(E^+ - E^-) = 0.22769$ is about 41% larger than the MC result $l = 0.16160 \pm 0.00047$ [21].

6 Conclusion

We have proposed a self-consistent TPVA, which gives the optimized tensor product state for 3D classical systems, by way of the self-consistent improvement of the local tensors. Since the method finds out the best variational state without using a priori knowledge of the system, the self-consistent TPVA is applicable for various 3D models described by short range interactions.

To generalize the self-consistent TPVA to 2D quantum systems is a next subject that one might consider. This generalization is not trivial, since we have used the specific property of 3D classical systems when we obtain the self-consistent equation.

Acknowledgements

T. N. thank to G. Sierra and M.A. Martín-Delgado for the discussion about the tensor product state at CSIC. K. O. is supported by JSPS Research Fellowships for Young Scientists. This work was partially supported by the "Research for the Future" Program from The Japan Society for the Promotion of Science (JSPS-RFTF97P00201) and by the Grant-in-Aid for Scientific Research from Ministry of Education, Science, Sports and Culture (No. 09640462 and No. 11640376). Most of the numerical calculations were done by Compaq Fortran on the HPC Alpha21264 Linux workstation.

References

[1] S.R. White, *Phys. Rev. Lett.* **69** (1992) 2863.

[2] S.R. White, *Phys. Rev.* **B48** (1993) 10345.

[3] *Density-Matrix Renormalization — A New Numerical Method in Physics,* Lecture notes in Physics, eds. I. Peschel, X. Wang, M. Kaulke, and K. Hallberg (Springer Verlag, 1999).

[4] K. Hallberg, cond-mat/9910082.

[5] S. Liang and H. Pang, *Phys. Rev.* **B49** (1994) 9214.

[6] T. Nishino and K. Okunishi, *J. Phys. Soc. Jpn.* **68** (1999) 3066.

[7] T. Nishino, *J. Phys. Soc. Jpn.* 64 (1995) 3598.

[8] T. Nishino and K. Okunishi, *J. Phys. Soc. Jpn.* **65** (1996) 891.

[9] T. Nishino and K. Okunishi, *J. Phys. Soc. Jpn.* **66** (1997) 3040.

[10] A.L. Talapov and H.W.J. Blöte, *J. Phys. A, Math. Gen.* **29** (1996) 5727.

[11] A.M. Ferrenberg and D.P. Landau, *Phys. Rev.* **B44** (1991) 5081.

[12] I. Peschel and M.-C. Chung, cond-mat/9906224.

[13] S. Östlund and S. Rommer, *Phys. Rev. Lett.* **75** (1995) 3537; S. Rommer and S. Östlund, *Phys. Rev.* **B55** (1997) 2164.

[14] G. Sierra and M.A. Martín-Delgado, cond-mat/9811170.

[15] H. Niggemann, A. Klümper and J. Zittartz, *Z. Phys.* **B104** (1997) 103.

[16] Y. Hieida, K. Okunishi and Y. Akutsu, *New J. Phys.* **1** (1999) 7.

[17] H.A. Kramers and G.H. Wannier, *Phys. Rev.* **60** (1941) 263.

[18] K. Okunishi and T. Nishino, cond-mat/9909097.

[19] R. B. Potts, *Proc. Camb. Phil. Soc.* **48** 106.

[20] R.J. Baxter, *Exactly Solved Models in Statistical Mechanics* (Academic Press, London, 1982).

[21] W. Janke and R. Villanova, *Nucl. Phys.* **B489** (1997) 679.